ELSEVIER

Biophysical Chemistry 113 (2005) 275–288

Biophysical Chemistry

www.elsevier.com/locate/bpc

Automated oncogene detection in complex protein networks with applications to the MAPK signal transduction pathway

Dhruv Pant, Avijit Ghosh*

Drexel University, 3141 Chestnut st, Philadelphia, PA, 19104, United States

Received 3 August 2004; accepted 10 September 2004
Available online 18 October 2004

Abstract

Activation of the extracellular signal-regulated kinases (ERK1/2; p42/p44 mitogen-activated protein kinase (MAPK)) is one of the most extensively studied signaling pathways not least because it occurs downstream of oncogenic RAS. Here, we take advantage of the wealth of experimental data available on the canonical RAS/RAF/MEK/ERK pathway of Bhalla et al. to test the utility of a newly developed nonlinear analysis algorithm designed to predict likelihood of cellular transformation. By using ERK phosphorylation as an "output signal", the method analyzes experimentally determined kinetic data and predicts putative oncogenes and tumor suppressor gene products impacting the RAS/MAPK module using a purely theoretical approach. This analysis identified several modifiers of ERK/MAPK activation described previously. In addition, several novel enzymes are identified which are not previously described to affect ERK/MAPK phosphorylation. Importantly, the nonlinear analysis enables a ranking of modifiers of MAPK activation predicting their relative importance in RAS-dependent oncogenesis. The results are compared with a linearized analysis based on sensitivity analysis about the steady state or metabolic control analysis (MCA). The results are favorable, pointing to the utility of first-order sensitivity analysis and MCA in the analysis of complex signaling networks for oncogenes.
© 2004 Elsevier B.V. All rights reserved.

Keywords: Oncogene detection; MAPK signaling; Nonlinear analysis

1. Introduction

Intracellular signal transduction has been of interest to cancer researchers for many years based on the consideration that many oncogenes and suppressor genes affect signaling cascades. Only recently, however, it has been appreciated that signal transduction forms a complex network rather than being composed of linear and separate pathways. The net response of network activation governs normal cell growth and function by control of gene expression, a process that can lead to cell proliferation, arrest or death [1,2]. Mutant proteins situated at critical nodal points can be expected to affect multiple pathways and are likely to contribute to neoplastic transformation. Mutational events may affect protein function through modulation of enzymatic activity [3–5] or by affecting protein stability and, thus, steady-state expression levels [6,7].

The nonlinear nature of signaling cascades necessitates novel tools to dissect their complexity. Here, we describe a computational method that enables the analysis of complex networks with the intent of identifying enzymes of relevance to the transformed state. As a first step in testing the robustness of this approach, we made use of a large body of data on the canonical RAS/RAF/MEK/ERK pathway accrued experimentally over many years. We demonstrate that the model predicts several candidates for mutational events likely to contribute to transformation. In addition, several nonobvious candidates are identified that warrant future experimental exploration.

The theoretical model chosen upon which to base this study is one of several highly regarded computational

* Corresponding author. Tel.: +1 215 8952726; fax: +1 215 8955934.
E-mail address: avijit@physics.drexel.edu (A. Ghosh).

0301-4622/$ - see front matter © 2004 Elsevier B.V. All rights reserved.
doi:10.1016/j.bpc.2004.09.004

studies of this central cascade. Recent studies of the mitogen-activated protein kinase (MAPK) signal transduction pathway have been developed by Schoeberl et al. [8], Kholodenko [9], Levchenko et al. [10] as well as others. The canonical MAPK pathway includes several major networks including PLC, PLC-γ, PLA2, PKC, Ras and calcium sequestering channels developed by Bhalla and Iyengar [11]. This network has several positive and negative feedback loops, multiple steady states and exhibits highly nonlinear behavior even within this subnetwork within the cell [11]. The interplay between the positive and negative feedback loops, attenuation and stimulatory factors all play a crucial role in the transformation of this central cascade.

2. Computational methods

The basis for discovering how certain mutations will affect the signaling behavior using a computational systems biology approach necessitates in first having an experimentally validated numerical model of the functioning signal transduction pathway. The parameters for the model of the functioning signal transduction network are taken from the pioneering work of Bhalla and Iyengar [11]. While the validation of certain features such as the proposed feedback loop remain to be tested, as the overall features of Bhalla and Iyengar's [11] kinetic model reproduce experimentally determinable behavior, it provides a reasonable test suite upon which to test the computational approach, with the acknowledgment that any refinements or corrections to the model will require a necessary correction in the analysis. Currently, the analysis does not include the negative feedback loop through MKP recently described by Bhalla et al. [12]. As this loop is not coupled to any members of the signaling pathway outside of ERK and MKP, this feedback loop is expected to have the same effect on mutations of upstream members. For this reason, the overall ranking (except for mutations directly in MKP and ERK) of enzymes provided by this analysis is expected to be the same, with an understanding that there would be a common attenuation effect on ERK of all mutations from this proposed negative feedback loop.

The goal here is to use energetic considerations of mutations to perform a nonlinear analysis of perturbations in the signaling process. The model derived by Bhalla et al. has been tested extensively against experimental data and is available publicly at the *cellml* website [13]. We emphasize that, while our own implementation is different from the implementation using the *Genesis* code base developed by Bhalla et al. [14], both the parameters and coupled set of elementary reactions are the same. Like *Genesis*, the numerical implementation and scripts necessary to reproduce the results of the mutational studies are available freely under the Gnu Public License with source code and binaries [15].

The complete cellular model is broken down into three localized compartments: the extra-cellular matrix, the cytosol and the calcium sequestering endosomal regions. Elementary chemical reactions describe the enzymatic and non-enzymatic reactions within each compartment. These reactions may be written as:

$$\sum_i n_i R_i \underset{k_b}{\overset{k_f}{\rightleftharpoons}} \sum_j n_j P_j \tag{1}$$

where a set of reactant species R_i with stoichiometric coefficients n_i interconverts into a set of product species P_j, with stoichiometric coefficients n_j with rate constants k_f and k_b. As collisions that are greater than bimolecular are rare, typically the order of an elementary chemical reaction is not greater than 2. Characteristics of signaling pathways are enzymatic reactions such as phosphorylation or dephosphorylation events. These reactions may be expressed as a combination of a reversible and a irreversible chemical reaction as follows:

$$E + S \underset{k_1}{\overset{k_2}{\rightleftharpoons}} E.S \xrightarrow{k_3} E + S^* \tag{2}$$

E represents an enzyme which catalyzes the substrate S. The intermediate species $E.S$ first forms reversibly with rate constants k_1 and k_2 followed by an irreversible catalytic step with rate constant k_3 which releases the activated substrate S^* and the enzyme for further catalysis.

One may express the time rate of change in concentration of *all* species in the complex, nonlinear cascade of reaction pathways as a coupled set of ordinary differential equations (ODEs), Eq. (3). The time rate of change of any species A is given as the sum of the time rate of change of that species involved in all of its elementary reactions of type Eq. (1). The change in concentration of any species C_i in a system of unimolecular and bimolecular reactions may then be written out as

$$\frac{d[C_i]}{dt} = \sum_j k_{ij}[C_j] + \sum_{l>m} k_{ilm}[C_l][C_m] + \sum_j T(C_i, C_j) \tag{3}$$

where k_{ij} is the rate constant for a unimolecular reaction involving species C_i and C_j at concentrations $[C_i]$ and $[C_j]$, respectively. If k_{ilm} is positive then k_{ilm} represents the rate constant of formation of species C_i from a bimolecular reaction between species C_l and C_m with concentrations $[C_l]$ and $[C_m]$. Conversely, if k_{ilm} is negative, then k_{ilm} represents the rate constant of disassociation of species C_i into two species C_l and C_m. $T(C_i,C_j)$ represents a function governing the passive transport of a species C_i into a

different compartment at which time it is labeled with a subscript j as C_j.

In the current signal transduction model, only Ca^{2+} is transported across compartments passively. The direction of transport is dependent simply on the difference in concentrations across the membrane. Letting Ca_a^{2+} represent calcium in compartment A and Ca_b^{2+} represent calcium in compartment B, then the time rate of change in concentration of each species (used in $T(C_i,C_j)$) may be expressed as:

$$V_b \frac{d[Ca_b^{2+}]}{dt} = P([Ca_a^{2+}] - [Ca_b^{2+}]) \quad (4)$$

$$V_a \frac{d[Ca_a^{2+}]}{dt} = -P([Ca_a^{2+}] - [Ca_b^{2+}]) \quad (5)$$

where P is the permittivity constant multiplied by the area of the membrane region (assumed to be a constant throughout the simulation) and V_a and V_b are the volumes of compartment A and B, respectively.

The spatial dependence of the concentrations of the proteins within a compartment is ignored in the kinetic model developed by Bhalla and Iyengar [11] and correspondingly in the one used in our computational study. This may be described as the 'well-stirred' approximation. It is assumed that the concentrations of all the proteins are uniform throughout the explicitly defined compartment and that no concentration gradients exist within that region. A mutation in a particular gene in a signaling pathway manifests itself in one of two ways. In the first case, the mutation may directly affect the *interaction* between two species. If two species A and B reversibly associate/disassociate with rate constants k_f/k_b:

$$A + B \underset{k_b}{\overset{k_f}{\rightleftharpoons}} A.B \quad (6)$$

then a mutation of this type will perturb k_f or k_b by some amount. For instance, lowering k_f by some amount represents a mutation that hinders the ability of species A or B to associate into $A.B$. We define a mutation of this type as an "interaction" mutation. This mutation may occur in either species A or B, as the effect is the same. In some cases, a particular enzyme may interact with multiple partners. This makes the mutation non-symmetric. Consider a mutation that affects the association rate between PP2-A and phosphorylated Raf (Raf*). A mutation in Raf may affect the PP2-A and Raf* interactions without affecting any other interaction. However, as the kinetics and mechanism of PP2-A on its interacting partners are similar, a mutation in a dominant subunit of PP2-A affects all interactions of PP2-A and its partners in the MAPK pathway. For this reason, some interaction mutations are considered to be "group interaction mutations." The list of group interaction mutations is shown in Table 1.

Arrhenius theory may be used to connect the rate of barrier crossing k_f to the barrier energy. The rate of interconversion from reactant to product may be given as:

$$k_f = Ae^{-E_a/k_bT} \quad (7)$$

where A is a constant prefactor, E_a is the barrier energy of activation and k_b is Boltzmann's constant. Mutations in the enzyme may affect a transition rate by either increasing the barrier height or changing the free energy of the initial state

Table 1
Listing of the "group interaction" reactions

No.	Reaction	X
1	X*+PP2A⇌X*−PP2A X*−PP2A→PP2A+X	X*: Raf*, Raf**, MEK*, MEK**
2	X*+MKP1⇌X*−MKP1 X*−MKP1→MKP1+X	X*: ERK*, ERK_{tyr}*
3	PKC(g)+GAP⇌PKC(g)−GAP PKC(g)−GAP→PKC(g)+GAP*	PKC(g): PKC-DAG-AA*, PKC-Ca-AA*, $PKC\text{-}DAG_{memb}$, PKC_{basal}*, PKC-AA*, $PKC\text{-}Ca^*_{memb}$
4	PKC(g)+GEF⇌PKC(g)−GEF PKC(g)−GEF→PKC(g)+GEF*	PKC(g): PKC-DAG-AA*, PKC-Ca-AA*, $PKC\text{-}DAG_{memb}$, PKC_{basal}*, PKC-AA*, $PKC\text{-}Ca^*_{memb}$
5	PKC(g)+Raf⇌PKC(g)−Raf PKC(g)−Raf→PKC(g)+Raf*	PKC(g): PKC-DAG-AA*, PKC-Ca-AA*, $PKC\text{-}DAG_{memb}$, PKC_{basal}*, PKC-AA*,$PKC\text{-}Ca^*_{memb}$
6	GDP−Ras+GEF(g)*⇌GDP−Ras−GEF(g)* GDP−Ras−GEF(g)*→GEF(g)*+GTP-Ras	GEF(g)*: CaM-GEF, GEF*, Gβγ-GEF
7	X+MEK**⇌X−MEK** X−MEK**→MEK**+X*	X: ERK, ERK_{tyr}*
8	X+Raf−GTP−Ras*⇌X−Raf−GTP−Ras* X−Raf−GTP−Ras*→Raf−GTP−Ras*+X*	X: MEK, MEK*

PKC has six activated isoforms, shown in column 3, each of which interact with GAP, GEF and Raf with the same kinetics. Similarly, GEF has three activated isoforms.

of the system by some amount ΔE. The new mutated system may therefore be considered to be a perturbed system with a new barrier of height E'_a and a forward transition rate of k'_f (Fig. 1).

The ratio k'_f/k_f is:

$$k'_f/k_f = \frac{e^{-(E_a+\Delta E)/k_b T}}{e^{-E_a/k_b T}} \tag{8}$$

and simplifying

$$k'_f/k_f = e^{-\Delta E/k_b T} \tag{9}$$

The right side of Eq. (9) is a function of the *change* in the barrier height and not of the barrier height E_a itself. Given two elementary reactions:

$$A \overset{k_{f_1}}{\rightleftharpoons} B \tag{10}$$

$$C \overset{k_{f_2}}{\rightleftharpoons} D \tag{11}$$

with barrier heights E_1 and E_2. A perturbation of the barrier energies by the same amount ΔE leads to the following relation:

$$k'_{f_1}/k_{f_1} = k'_{f_2}/k_{f_2} = e^{-\Delta E/k_b T} \tag{12}$$

The relative kinetic rates are affected as a ratio (k_{mod}) rather than as an absolute:

$$k_{mod} \equiv e^{-\Delta E/k_b T} \tag{13}$$

$$k'_{f_1} = k_{mod} k_{f_1} \tag{14}$$

Another kind of mutation, defined here as an "expression-level mutation", may also cause a change in the initial concentration of a particular protein in the signaling pathway. These mutations may occur when a mutation in a gene causes a change in the basal level of that protein, for example, by gene amplification or gene deletion events.

Expression-level mutations may be described by considering a simple precursor model that forms species A. (Conversely, regulatory pathways which downgrade A may be considered as well)

$$\text{precursor} \overset{k_f}{\underset{k_b}{\rightleftharpoons}} A \tag{15}$$

At equilibrium, the following condition holds:

$$k_f/k_b = [A]/[\text{precursor}] \tag{16}$$

$[A]$ is the concentration of species A and [precursor] is the multiplied concentrations of any buffered precursor species in the cell. Combining Eqs. (7) and (16) for a "normal" system with a forward rate constant k_f and a "mutated" system with a forward rate constant of k'_f

$$k'_f/k_f = [A]'/[A] = e^{-\Delta E/k_b T} \tag{17}$$

yields

$$[A]' = k_{mod}[A] \tag{18}$$

Again, a *similar* mutation that changes a barrier by amount ΔE will affect the equilibrated initial concentration of the species involved in the signal transduction pathway as a ratio defined by k_{mod} (Eq. (14)) rather than an absolute change in the concentration. This allows one to examine mutations simply as a function of changes in either initial concentrations or rate constants in the normal protein network model. For each mutation or set of mutations, only equilibrated phosphorylated ERK (ERK*) levels are measured in our implementation although this approach is easily extensible to multiple responses.

Two methods are used for discovering how perturbations to the signaling pathway will effect signaling. As the system

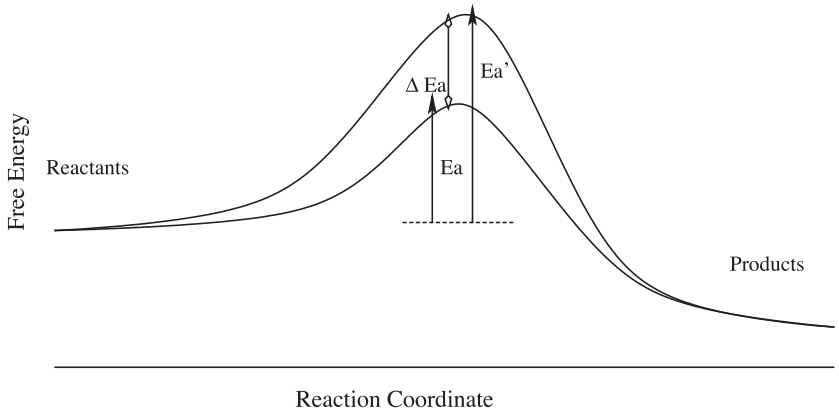

Fig. 1. Graphical representation of the energy barriers involved in a reaction. An increase in the barrier height lowers the rate constant. The lower rate constant k'_f corresponds to the greater barrier height E'_a.

is nonlinear, the effect of a mutation may only rigorously be found by systematically integrating out the full system of equations (Eq. (3)) describing the mutated signaling pathway and evaluating the response. For the system of 156 equations representing the MAPK pathway (represented schematically in Fig. 2), the response of any single mutation on a system may be calculated easily on a PC workstation using stiff integrators.

The computational approach is similar to metabolic control analysis (MCA), except that, as the perturbations (Eq. (14)) are not necessarily small, it is necessary to numerically integrate out the new system to detect whether a transition to a new "proliferative" steady state is reached due to a particular mutation. It is however useful to compare this direct analysis with the results obtained from sensitivity analysis around the steady state. Such an approach will become useful when for instance the number of simultaneous mutations in the system increases and direct simulation may no longer be tractable.

For this reason, an approximate method based on sensitivity analysis using linear response theory is also used. The results from sensitivity analysis are compared to the more robust method which measures the actual response. In the linear approximation (described more fully below), the change in [ERK*] in response to a particular relative perturbation M is simply proportional to $\Delta[\mathrm{ERK}]/\Delta M$. The linearized form is proportional to that used in sensitivity analysis. This approach is similar in spirit to a recently developed "modular framework" of Kholodenko et al. [16,17]. In this framework, steady-state responses of a

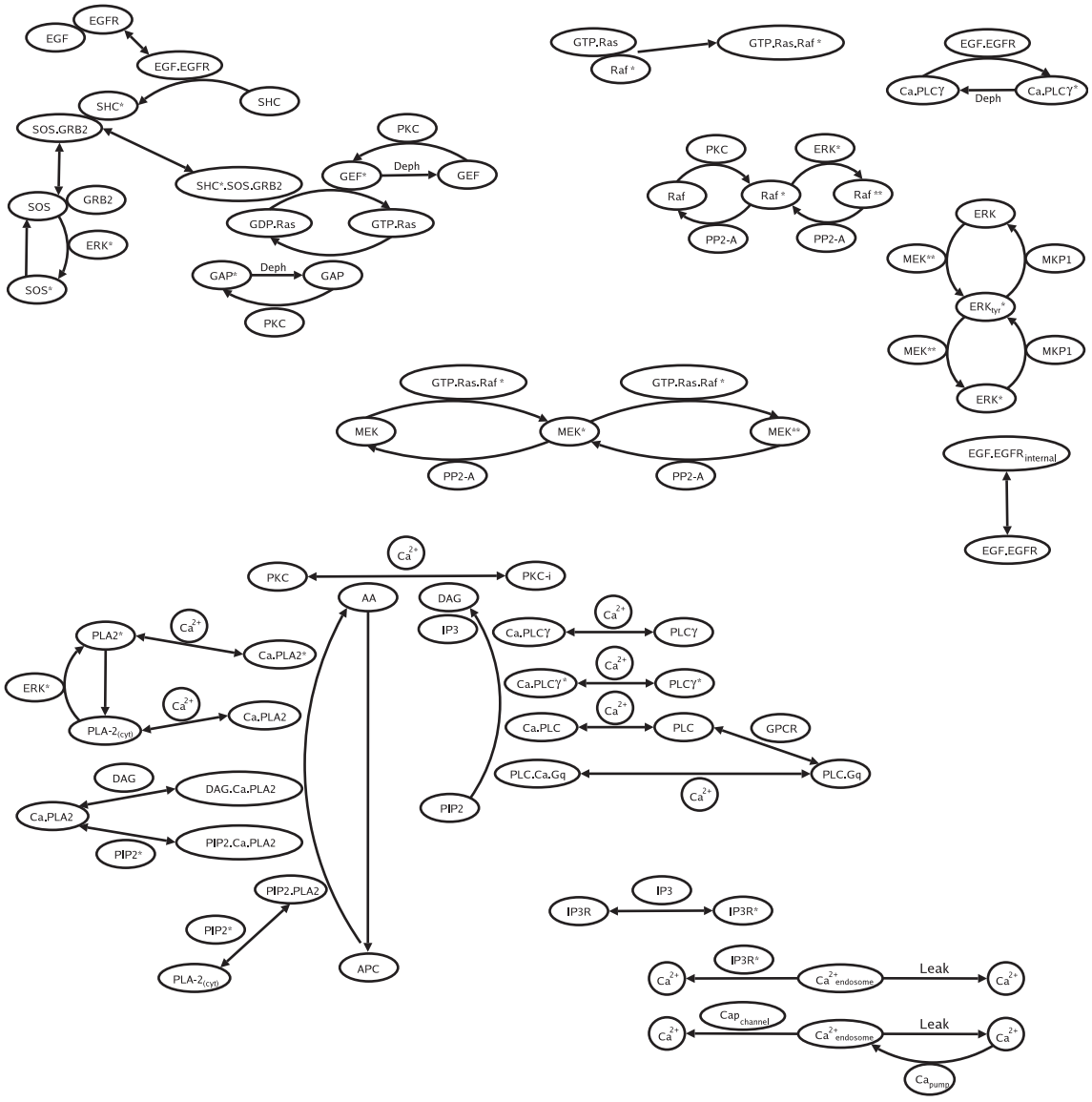

Fig. 2. The main pathways used in this model. The arcs connect species involved in enzymatic (such as phosphorylation/dephosphorylation) reactions. For example, PIP2 conversion to DAG and IP3 is carried out by four enzymes: Ca.PLC, Ca.Gα-GTP.PLC, Ca.PLCγ and Ca.PLCγ*. The association, disassociation reactions are shown by straight arrows. In the figure, Gq≡Gα-GTP.

interaction network are analyzed in terms of local and global responses.

For the direct, nonlinear analysis, we systematically measure the total response (that is any transitions to a new proliferative steady state) of the system to any single mutation using the algorithm shown in Fig. 3.

k_{mod} represents the effect of a change in the energy of activation (Eq. (14)). $B_{k_{\mathrm{mod}}}$ is the set of all mutations that activate ERK at a particular value of k_{mod}.

At k_{mod}=1, the system is a normally functioning signal pathway. At perturbations of k_{mod} away from unity, certain mutations will cause ERK phosphorylation. These mutations are ranked as a function of k_{mod} (equivalently, the change in energetic barrier height caused by the mutation).

The oncogenic transformation process may not expected to be the result of a single mutation process even within the set of interacting enzymes explicitly modeled (Fig. 2). In investigating the role of multiple simultaneous mutations within the central MAPK network, the algorithm shown in Fig. 3 will remain essentially the same with the following extension. In the box tagged (1), set A is extended to include all sets of mutations. In the area tagged (2), I is now an instance of a particular set of simultaneous mutations. The analysis of multiple mutations will be part of a subsequent manuscript.

The nonlinear analysis is then compared to a linear response approach based upon sensitivity analysis and metabolic control analysis [18–20]. In this approach, one

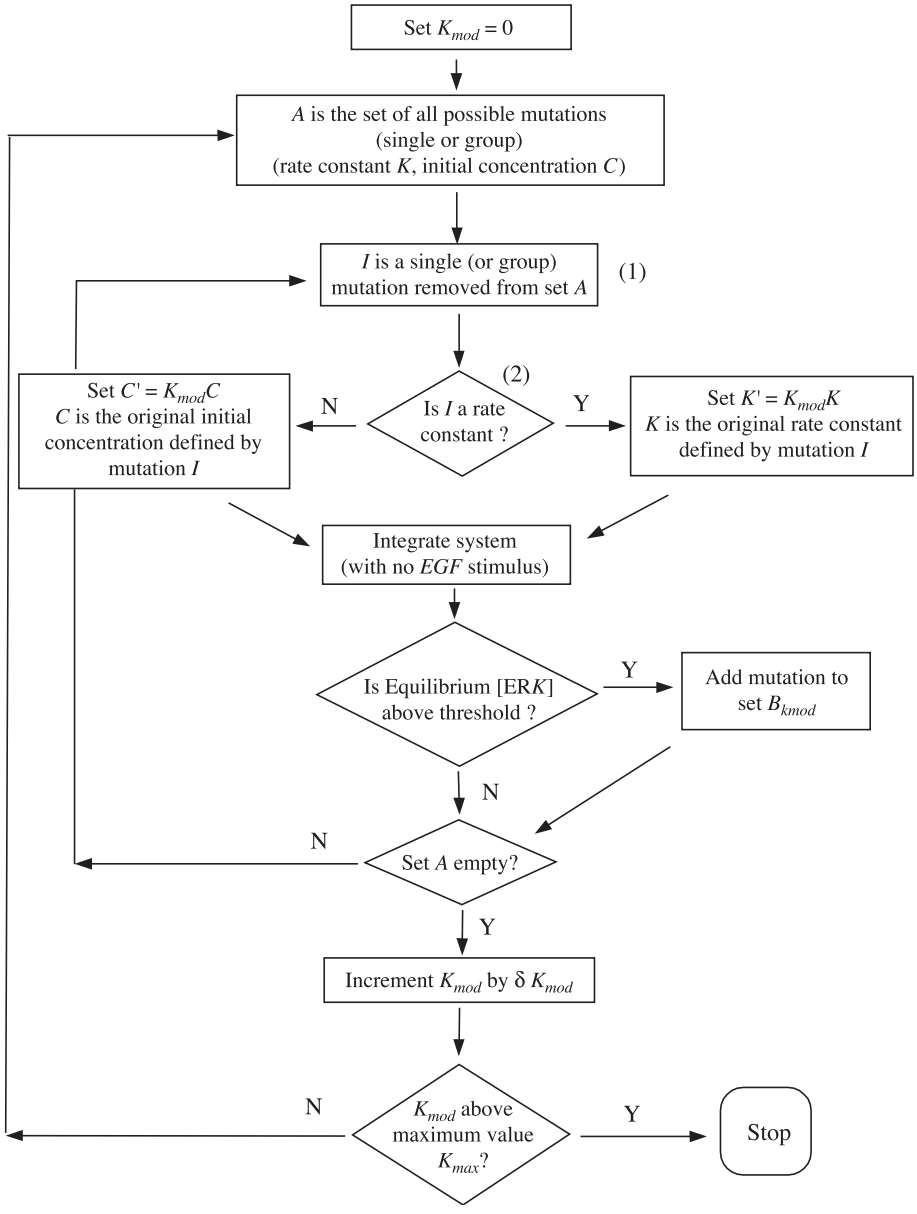

Fig. 3. Analysis flowchart.

simplifies the complex system of nonlinear equations by assuming the response of ERK to small changes (Δk_i) is essentially linear at steady state:

$$\mathrm{ERK}(k_i + \Delta k_i) = \mathrm{ERK}(k_i) + D_i \Delta k_i \tag{19}$$

with D_i defined as d[ERK]/dk, the response L_i to a *relative* change (Eq. (14)) in k_i may be defined as

$$L_i \equiv \frac{\Delta[\mathrm{ERK}]}{\Delta k_i / k} = \frac{\Delta[\mathrm{ERK}]}{\Delta k_{\mathrm{mod}}} \tag{20}$$

L_i may be used to rank the response and may be calculated numerically or analytically. It is interesting to note that L_i is proportional to the *sensitivity parameter* S_i used in the analysis of nonlinear dynamics. The *sensitivity* of an output (ERK concentration) with respect to a parameter (k_i) is defined as:

$$S_i = \frac{\mathrm{d}\log[\mathrm{ERK}]}{\mathrm{d}\log(k_i)}$$

$$= \frac{\mathrm{d}[\mathrm{ERK}]/[\mathrm{ERK}])}{\mathrm{d}k_i/k_i}$$

$$= \frac{\Delta[\mathrm{ERK}]/[\mathrm{ERK}]}{\Delta k_i/k_i} \tag{21}$$

where Δ[ERK] is the change in ERK concentration in response to a change in k_i by an amount Δk_i and [ERK] and k_i are the nonperturbed steady-state ERK concentrations and the normal unmutated rate constant, respectively.

As steady-state [ERK] is constant, the rankings using sensitivity analysis S_i are directly proportional to the linear response approach L_i. It is expected then, that rankings based on sensitivity analysis are expected to be the same as our linearization. More specifically, first-order sensitivity analysis about the steady state may be described more fully as metabolic control analysis [20–24]. The derivation above motivates the use of nondimensional units in ranking physically relevant quantities such as mutation efficacy in aberrant signaling and compares to the nonlinear approach described previously.

In the general case, as the system in inherently complex and nonlinear, there is no guarantee that a linear approximation is correct for evaluating a nonlinear set of differential equations of the form of Eq. (3), so systematic measurement (Fig. 3) must be used as a point of comparison.

3. Results

The signal transduction model of a normally functioning pathway is comprised of a coupled set of ordinary differential equations derived from 152 separate elementary chemical reactions, 4 channel equations and 238 rate constants. The reactions are built from both enzymatic and nonenzymatic reactions (Fig. 2).

As a special case, the system can be perturbed by completely removing a single interaction between two species by setting k_{mod}=0. For interaction mutations, at k_{mod}=0, the species involved no longer participate in that particular reaction. For expression-level mutations, that species will no longer participate in the signaling network, this latter case being analogous to a gene knockout experiment. k_{mod}<1 implies that interaction mutations are "inhibiting" and expression-level mutations are underexpressed. Conversely, k_{mod}>1 implies that interaction-level mutations are "activating" and expression-level mutations are overexpressed.

In a normally functioning signal pathway, the steady state concentration of phosphorylated ERK is 0.00015 μM at equilibrium. By perturbing certain parameters—expression levels or particular rate constants—the modified set of coupled equations will give rise to finite concentrations of activated ERK in the absence of EGF. A threshold of 0.02 μM is used to gauge whether significant phosphorylation has occurred. This threshold is arbitrary, but set high enough such that detection of activated states is clearly defined. Each run is carried out until steady state with each run taking about 0.5 s on a single processor of a 2.66-GHz dual xeon system using a 4th-order Rosenbrock stiff integrator.

For a single mutation, at k_{mod}=0, 52 interaction mutations cause ERK phosphorylation. The list is given in Table 2.

In Fig. 4, the ERK responses to these perturbations are overlayed. In the standard pathway, several mechanisms attenuate signaling to prevent proliferative stimulation (Fig. 2). Endocytosis serves to attenuate further signaling. In a feedback mechanism, phosphorylated ERK phosphorylates SOS preventing binding to GRB2. PP2-A and MKP both serve as phosphatases to each phosphate site on RAF, MEK and ERK. The messenger Inositol 1,4,5-trisphosphate (IP3), central to the release of sequestered calcium, is converted to Inositol. Arachidonic acid (AA), central to stimulation of PKC, is eventually converted to APC (arachidonoyl–phosphatidylcholine). These attenuation factors are balanced by several stimulatory mechanisms. Direct stimulation may occur by EGFR through both PLC-γ and SHC. Calcium bound PLC-γ stimulates DAG and IP3 production. DAG serves to stimulate the central positive feedback loop governed by PKC and IP3 in turn releases more calcium in a parallel positive feedback mechanism. The first feedback loop is governed by ERK stimulation of PLA2 which, upon binding with calcium and DAG, activates PKC which stimulates the MAPK cascade by phosphorylating GEF as well as Raf directly. The interplay between the attenuation processes and the stimulatory mechanisms are highly nontrivial and will be discussed in some detail below.

Phosphorylated ERK levels can be significant in these pathways reaching levels of about 0.35 μM in certain

Table 2
Total of 52 reactions which activate ERK when that interaction is fully inhibited (k_{mod}=0)

Reaction	Dir
Ca−PLA2+PIP2*⇌PIP2−Ca−PLA2	b
Ca−PLA2+DAG⇌DAG−Ca−PLA2	b
APC+PIP2−Ca−PLA2⇌APC−PIP2−Ca−PLA2	b
ERK_{tyr}*+MKP1⇌ERK_{tyr}*−MKP1	f
Raf+PKC−Ca^*_{memb}⇌Raf−PKC−Ca^*_{memb}	b
PLA2*→PLA2−cyt	f
PLA2*+Ca⇌Ca−PLA2*	b
ERK+MEK**⇌ERK−MEK**	b
GDP−Ras+Gβγ−GEF⇌GDP−Ras−Gβγ−GEF	b
IP3R+IP3+IP3+IP3⇌IP3R*	b
Ca_{transp}+Ca+Ca⇌Ca2−Ca_{transp}	f
Ca2−Ca_{transp}→Ca_{transp}+Ca_{Stores}+Ca_{Stores}	f
Ca_{Stores}+Ca_{Stores}+Cap−Chan*⇌Cap−Chan	f
PIP2+Ca−PLC⇌PIP2−Ca−PLC	b
Gα−GDP+Gβγ→Gαβγ	f
GAP+PKC−DAG−AA*⇌GAP−PKC−DAG−AA*	b
PIP2+Ca−PLCγ⇌PIP2−Ca−PLCγ	b
PLC+Ca⇌Ca−PLC	b
Ca−Gα−GTP−PLC→Gα−GDP+Ca−PLC	f
ERK_{tyr}*−MKP1→ERK+MKP1	f
MEK+GTP−Ras−Raf*⇌MEK−GTP−Ras−Raf*	b
PIP2+Ca−Gα−GTP−PLC⇌PIP2−Ca−Gα−GTP−PLC	b
Raf+PKC−DAG−AA*⇌Raf−PKC−DAG−AA*	b
GEF+Gβγ⇌Gβγ−GEF	b
Ca+Ca_{pump}⇌Ca−Ca_{pump}	f
Ca−Ca_{pump}→Ca_{ext}+Ca_{pump}	f
GEF*→GEF	f
$PKC_{cytosolic}$+Ca⇌Ca−PKC	b
GDP−Ras+GEF*⇌GDP−Ras−GEF*	b
Raf*+PP2A⇌Raf*−PP2A	f
Raf*−PP2A→Raf+PP2A	f
DAG→PC	f
$PKC_{cytosolic}$+DAG⇌DAG−PKC	b
Ca−PKC+DAG⇌DAG−Ca−PKC	b
DAG−PKC+AA⇌AA−DAG−PKC	b
AA→APC	f
GTP−Ras−GAP→GDP−Ras+GAP	f
GAP*→GAP	f
GTP−Ras+GAP⇌GTP−Ras−GAP	f
DAG−Ca−PKC⇌PKC−DAG*$_{memb}$	b
Ca−PKC+AA⇌PKC−Ca−AA*	b
$PKC_{cytosolic}$+AA⇌PKC−AA*	b
AA−DAG−PKC⇌PKC−DAG−AA*	b
Ca−PKC⇌PKC−Ca^*_{memb}	b
$PKC_{cytosolic}$⇌PKC_{basal}	b
MEK*+GTP−Ras−Raf*⇌MEK*−GTP−Ras−Raf*	b
MEK*−PP2A→MEK+PP2A	f
MEK*+PP2A⇌MEK*−PP2A	f
Raf*+GTP−Ras⇌GTP−Ras−Raf*	b
MEK**−PP2A→MEK*+PP2A	f
MEK**+PP2A⇌MEK**−PP2A	f
ERK*−MKP1→ERK_{tyr}*+MKP1	f
ERK*+MKP1⇌ERK*−MKP1	f

The second column indicates the direction of the mutation, whether the mutation occurs in the forward (f) or backward (b) direction.

cases. It is much more likely that a random mutation will simply modify the barrier height as shown in Fig. 1 by some amount ΔE in a manner described by Eq. (9). In this case, interaction mutations lead to reactions which still interact and expression-level mutations will result in a change in the basal level of the enzyme. This more general case is evaluated by measuring the response to a single mutation of values k_{mod} from 0 to 1 in increments of δk_{mod}=0.05.

In all cases, mutations which cause significant ERK phosphorylation at small changes in the barrier height continue to do so at larger perturbations. This allows one to rank each mutation as a function of the smallest value of k_{mod} which still causes ERK phosphorylation. The chief hypothesis in this ranking is that enzymes which may cause phosphorylation with smaller changes in the barrier height of activation are more amenable to transforming the pathway with smaller random mutations and are therefore more likely to be oncogenes or tumor suppressor genes. The full sets of rankings are tabulated in Tables 3 and 4. Table 3 ranks inhibiting interaction mutations, while Table 4 ranks activating interaction mutations.

To gauge the robustness of this method, the rankings provided in Tables 3 and 4 were compared to known oncogenes found in the literature.

In Table 3, inactivation of PP2-A causes ERK activation at any k_{mod} value lower than 0.75, while the next highest ranked interaction mutation GTP–Ras is unable to activate ERK until k_{mod} is lower than 0.6. By far, the phosphatase PP2-A appears to be the single most important modifier of ERK phosphorylation. Motivated by the fact that okadaic acid is a strong tumor promoter as well as an inhibitor of PP2-A, mutations in subunit A of PP2-A have recently been found to be expressed in lung, colon tumors as well as in breast cancers and certain melanomas [25–27]. Biologically, the key role that PP2-A plays in cellular transformation may be mitigated by the existence of isoforms of PP2-A as a single mutation in a subunit or isoform is in part compensated for by nonmutated species and may, in part, be an explanation for the existence of isoforms of enzymes at crucial junctures within cellular signal transduction networks.

The next mutation predicted is one that inhibits Raf GTP-Ras disassociation. This mutation is the third highest ranked in both the deactivating set and the activating set. In a mutation study by Cutler and Morrison [28], mutations in human Raf have been found which increase enzymatic and biological activity of Raf by allowing Raf to continue to signal even in the absence of Ras binding. The exact mechanism of malignant signaling in this portion of the pathway is different from the one predicted. Experimentally, Raf catalyzes MEK without Ras binding. As this interaction is not in the normal signaling model of Bhalla and Iyengar [11], this explicit interaction does not show up in the rankings. Nonetheless, the outcome—enhanced signaling through modified behavior of Raf—remains highly ranked, corresponding to the third highest ranked interaction in the activating set. This brings us to an important point: while the method attempts to find interactions that cause malignant signaling, the results from such a ranking hold

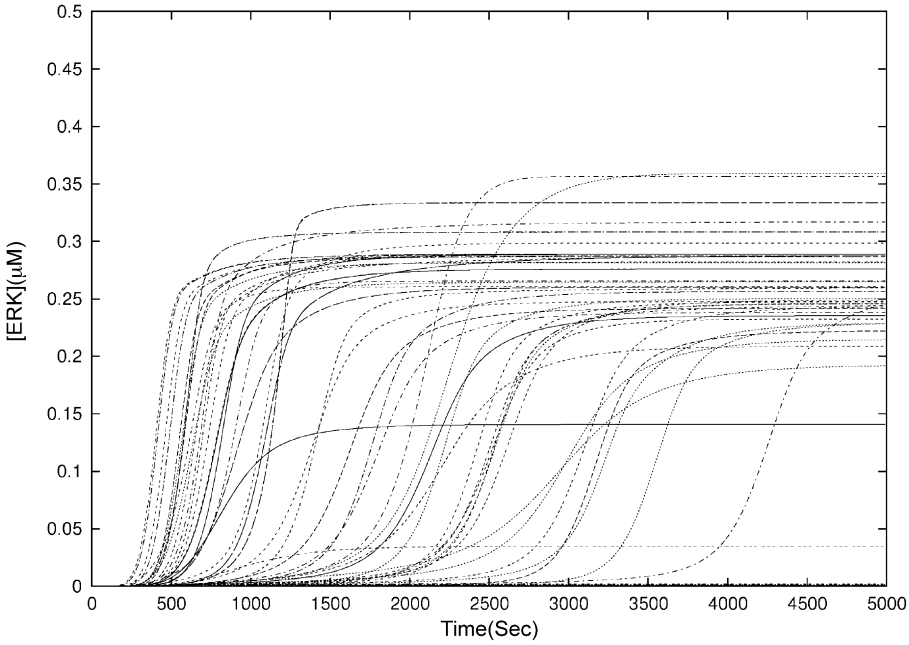

Fig. 4. Temporal evolution of activated ERK concentration for the 238 mutated pathways with an interaction fully inhibited (k_{mod}=0). Total of 52 of the mutated pathways cause elevated phosphorylated ERK levels, as shown. The concentration of activated ERK for the remaining 186 pathways is imperceptible.

for other similar mutations or pathways even when they are not explicitly mapped out.

In the fifth position of both Tables 3 and 4 is a mutation that inhibits the GTP.Ras GAP association. This interaction corresponds to the experimentally known mutation in residue 12 of Ras which inhibits Ras-GAP interactions [3,4]. The sixth ranked prediction in the deactivating set corresponds to inhibiting GTP hydrolysis. This predicted mutation is the well-known experimental mutation at residue 61 (Gln 61) in Ras which are known to inhibit GTP hydrolysis [4,5].

Mutations which regulate AA conversion to APC (arachidonoyl–phosphatidylcholine) occupy the seventh position in Table 3. AA plays an important role in mediating PKC stimulation of Raf. AA production has been linked to prostate cancer [29,30]. However, AA production has also

Table 3
Ranking of the "interaction" mutations based on the highest value of k_{mod} below which ERK activation occurs

Rank	k_{mod}	Reaction	Dir
1	0.75	X*+PP2A⇌X*−PP2A	f
2	0.75	X*−PP2A→PP2A+X	f
3	0.6	Raf*+GTP−Ras⇌Raf−GTP−Ras*	b
4	0.55	Raf*+PP2A⇌Raf*−PP2A	f
5	0.55	GTP−Ras+GAP⇌GTP−Ras−GAP	f
6	0.55	GTP−Ras−GAP→GAP+GDP−Ras	f
7	0.55	AA→APC	f
8	0.55	Ca−Ca_{pump}→Ca_{pump}+Ca_{ext}	f
9	0.5	X+Raf−GTP−Ras*⇌X−Raf−GTP−Ras*	b
10	0.5	Ca+Ca_{pump}⇌Ca−Ca_{pump}	f
11	0.5	Raf*−PP2A→PP2A+Raf	f
12	0.5	PKC−DAG−AA⇌PKC−DAG−AA*	b
13	0.5	PKC−DAG+AA⇌PKC−DAG−AA	b
14	0.5	DAG→PC	f
15	0.45	Raf+PKC(g)⇌Raf−PKC(g)	b
16	0.45	$PKC_{cytosolic}$+Ca⇌PKC−Ca	b
17	0.45	$PKC_{cytosolic}$+DAG⇌PKC−DAG	b
18	0.4	X*−MKP1→X+MKP1	f
19	0.4	GDP−Ras+GEF(g)*⇌GDP−Ras−GEF(g)*	b
20	0.4	MEK*+PP2A⇌MEK*−PP2A	f

These reactions represent the "inhibiting" set of mutations. Reactions with X (or X*) or (g) represent group reactions.

Table 4
Ranking of "interaction" mutations based on the lowest value of k_{mod} above which ERK activation occurs

Rank	k_{mod}	Reaction	Dir
1	1.35	X+PP2A⇌X−PP2A	b
2	1.6	Raf−GTP−Ras*+X⇌Raf−GTP−Ras*−X	f
3	1.65	Raf*+GTP−Ras⇌Raf−GTP−Ras*	f
4	1.7	Raf−GTP−Ras*−X→X*+Raf−GTP−Ras*	f
5	1.75	GTP−Ras+GAP⇌GTP−Ras−GAP	b
6	1.75	Raf+PKC(g)⇌Raf−PKC(g)	f
7	1.85	GEF(g)*+GDP−Ras⇌GDP−Ras−GEF(g)*	f
8	1.9	Raf*+PP2A⇌Raf*−PP2A	b
9	1.9	PKC−DAG−AA⇌PKC−DAG−AA*	f
10	1.95	PKC−DAG+AA⇌PKC−DAG−AA	f
11	2	GDP−Ras−GEF(g)*→GTP−Ras+GEF(g)*	f
12	2.1	Raf−PKC(g)→Raf*+PKC(g)	f
13	2.2	Ca+Ca_{pump}⇌Ca−Ca_{pump}	b
14	2.2	$PKC_{cytosolic}$+DAG⇌PKC−DAG	f
15	2.25	MEK*+Raf−GTP−Ras*⇌MEK*−Raf−GTP−Ras*	f
16	2.25	MEK**+X⇌X−MEK**	f
17	2.25	$PKC_{cytosolic}$+Ca⇌PKC−Ca	f
18	2.3	GDP−Ras+GEF*⇌GDP−Ras−GEF*	f
19	2.35	GAP+PKC(g)⇌GAP−PKC(g)	f
20	2.4	Ca−PKC⇌PKC−Ca*$_{memb}$	f

These reactions represent the "activating" set of mutations. Reactions with X (or X*) or (g) represent group reactions.

been linked to the inhibition of tumors. Many cancer preventative drugs, particularly COX-2 inhibitors, are known to induce apoptosis by stimulating the release of AA [31]. This points to the multiple roles which AA plays in cellular signaling and a reminder that one may not extrapolate too broadly from an analysis of just the MAPK-related pathways. Whether excessive AA may be linked to stimulation of the MAPK pathway through PKC in certain cancers is not currently known at the present time.

The next major prediction involves inhibition of calcium regulatory pathways, in effect increasing the amount of cytosolic calcium. Cytosolic Ca^{2+} mediates both PKC stimulation and PLA2 stimulation.

The link between calcium regulation and cancer is currently not well established. There is some evidence that elevation of calcium level has been linked to apoptosis of prostate cancer cells by mediating androgen receptor expression [32]. In the 6th and 12th place of Table 4 is PKC catalysis of Raf. This mutation shows up in the 15th place of Table 3.

Currently, the role of specific changes in PKC and oncogenesis is not completely well defined; however, there is evidence that abnormal posttranslational modifications of PKC are prevalent in thyroid tumors [33]. It remains to be seen whether PKC may also cause proliferation signals through the MAPK pathway via Raf signaling. It may be possible that this effect is again mitigated by the existence of PKC isoforms in a similar manner with PP2-A.

Phosphorylated GEF stimulates Ras signaling directly by removing GDP from inactive Ras–GDP. This class of mutations is currently unknown experimentally in tumor lines. In the 7th and 11th position of Table 4 and in the 19th position of Table 3, GEF catalysis of Ras–GDP is highly ranked.

Finally, in the 12th and 13th positions of Table 3 and in the 9th and 10th position of Table 4 are interactions involving phosphorylation of PKC. PKC stimulation of the MAPK pathway stimulates ERK directly and additionally provides amplified malignant stimulation through the PLA2 feedback network through MAPK activation of PLA2 back to PKC. To our knowledge, these specific mutations in PKC isoforms have not yet been identified in tumor lines except for the posttranslational mutations in PKC that has been found in thyroid cancer cited earlier [33].

In Table 5, the top 25 results obtained using linear response theory are ranked (Eq. (20)). One clear advantage of the linear response approach is the ability to give a much more precise ranking. Nonetheless, the similarity between Tables 3 and 5 is remarkable. As before, PP2-A (as a group interaction) shows up clearly on top, well separated from the rest of the possible mutations. The top six interactions in each table have the exact same predicted rankings.

The effect of changes in the expression level of proteins in the cell has also been examined using both approaches. The values of k_{mod} (Eq. (14)) perturb the expression level of each species in the cell. Of a possible 21 such mutations in the signaling pathway (Fig. 2), only a few cause ERK phosphorylation. The k_{mod} values used range from 0 to 4 in increments of Δk_{mod} of 0.05. As before, the k_{mod} value is a threshold value. The results of this analysis are tabulated in Table 6.

Table 5
A list of the 25 most significant reactions, as deduced from sensitivity analysis for the "inhibiting" mutations

Rank	Linear Response L_i	Reaction	Dir
1	0.001426	X*+PP2A⇌X*−PP2A	f
2	0.001141	X*−PP2A→PP2A+X	f
3	0.00067	Raf*+GTP−Ras⇌Raf−GTP−Ras*	b
4	0.00063	Raf*+PP2A⇌PP2A−Raf*	f
5	0.000629	GTP−Ras+GAP⇌GTP−Ras−GAP	f
6	0.000626	GTP−Ras−GAP→GAP+GDP−Ras	f
7	0.000564	X+Raf−GTP−Ras*⇌X−Raf−GTP−Ras*	b
8	0.000509	$Ca-Ca_{pump}\rightarrow Ca_{pump}+Ca_{ext}$	f
9	0.000507	Raf*−PP2A→PP2A+Raf	f
10	0.000501	Raf+PKC(g)⇌Raf−PKC(g)	b
11	0.000497	AA→APC	f
12	0.000458	GDP−Ras+GEF(g)*⇌GDP−Ras−GEF(g)*	b
13	0.000432	$Ca+Ca_{pump}\rightleftharpoons Ca-Ca_{pump}$	f
14	0.000408	DAG→PC	f
15	0.000406	$PKC_{cytosolic}+Ca\rightleftharpoons PKC-Ca$	b
16	0.000384	MEK**+PP2A⇌MEK**−PP2A	f
17	0.000368	PKC−DAG−AA⇌PKC−DAG−AA*	b
18	0.000368	MEK*+PP2A⇌MEK*−PP2A	f
19	0.000365	PKC−DAG+AA⇌PKC−DAG−AA	b
20	0.000349	X*+MKP1⇌X*−MKP1	f
21	0.000331	$PKC-Ca\rightleftharpoons PKC-Ca^*_{memb}$	b
22	0.000312	X*−MKP1→MKP1+X	f
23	0.000317	GAP*→GAP	f
24	0.000309	MEK**−PP2A→PP2A+MEK*	f
25	0.000306	X+MEK**⇌X−MEK**	b

Reactions with X (or X*) or (g) represent group reactions.

PKC ranks highest in the over-expressed enzymes, activating ERK through the MAPK pathway at a concentration which is predicted to be 1.4 times its concentration in the normal pathway. There is considerable experimental evidence connecting PKC over-expression and cancer in the literature. Using comparative genome hybridization techniques on 33 thyroid tumor DNAs and 2 tumor cell-lines, Chen et al. [34] found amplification of the gene encoding PKC-∈ to be amplified significantly in the tumor cell lines. Using positional cloning, Knauf et al. [33] also found amplification of PKC-∈ in 28% of thyroid neoplasms as well as in the WRO thyroid carcinoma cell line. In a study by Ref. [35], immortalized epithelial cells over-expressing PKCγ result in a fivefold increase in ERK 1/2 resulting in a similar increase in cyclin D1 leading to immortalization.

The next two over-expressed genes ranked are the well known Ras and Raf protooncogenes of the MAPK pathway. Ras and Raf have both been found to be overexpressed in TCR transgenic mice thymic lymphomas, ovarian caners, skin cancers, esophageal cancers and gastric carcinomas [36–42].

Raf overexpression has been found to confer immortalization to Rat-1 fibroblast lines by activating the MAPK

Table 6
Ranking of enzymes for overexpression and underexpression

k_{mod} (relative concentration)	Species overexpression	k_{mod} (relative concentration)	Species underexpression
1.4	$PKC_{cytosolic}$	0.7	PP2A
1.6	Raf	0.5	GAP
1.7	Ras	0.4	MKP1
1.7	$PLA2_{cytosolic}$		
1.9	GEF		
2.4	GPCR		
2.8	MEK		
3.0	PLC (PIP2 binding)		
3.4	PLCγ		
3.6	ERK		

The first and third columns indicate the relative concentration above which (for overexpression) or below which (for underexpression) ERK activation occurs. ERK activation is most sensitive to PKC overexpression and PP2A underexpression.

pathway [43]. There is also evidence that Raf overexpression conveys drug resistance in breast cancer [44].

PLA2 is predicted to be oncogenic when overexpressed at 1.7 times normal concentrations. PLA2 stimulates AA production in the cell which in turn activates PKC. Overexpression of PLA2 has been implicated in colorectal cancer [45]. In this study, tumor formation has been explicitly correlated with increased levels of AA, corresponding to the mechanism found by our procedure. Increased PLA2 expression levels have also been found in breast cancer and increased malevolence in prostate tumors [46,47].

The overexpression of G protein-coupled receptor (GPCR) is predicted to cause ERK activation when overexpressed at 2.4 times normal concentration levels. GPCR stimulates PLC which then stimulates DAG production. DAG in turn stimulates AA through PLA2. This particular pathway may be responsible for the mechanism of Kaposi's sarcoma-associated herpes virus which activates ERK and AKT via the PLC pathway [48].

MEK, a member of the MAPK signaling pathway is predicted to cause oncogenic transformation when overexpressed at 2.8 times normal concentrations. MEK has been found to be overexpressed in human renal cell carcinomas [49]. MEK has also recently been found to be overexpressed in metastatic prostate cancer as well breast carcinoma cells [50,51].

Overexpression of PIP2-specific PLC is predicted to cause ERK activation when overexpressed at three times normal concentrations. This enzyme has recently been implicated in the malignant transformation of gastric mucosa [52]. Finally, overexpression of PLC-γ, predicted to cause malignant transformation at 3.4 times normal concentrations, has been found in colorectal tumors in patients with familial adenomatous polyposis [53].

Of the genes predicted to cause malignant transformation when overexpressed, only ERK and Ras's GEF have not yet been shown to be overexpressed in tumor cells. As ERK and GEF mediate many signals, it is possible that overexpression of these genes causes apoptosis through pathways not covered by our simple model.

Of the underexpressed enzymes, the phosphatase PP2-A is the highest ranked prediction, causing ERK activation when PP2-A is underexpressed at 0.7 times normal concentration levels. Most tumor cells involving PP2-A involve alteration of one of the subunits [25,26]. However, there is evidence that gene deletion events have resulted in truncated PP2-A-β protein in colon tumors [27].

The next two expression-level mutations involve GAP and the MAPK phosphatase MKP. The p120 Ras GAP enzyme has not yet been found to be deleted or underexpressed in tumor lines. However, recently, a Rho family GAP protein has been found to be underexpressed in hepatocellular carcinoma [54]. The role of MKP-1 in tumor progression is more complex. It has been found to be overexpressed the early stages of prostate, colon and bladder cancer and with progressive loss of expression in later stages of tumor progression and in metastases [55]. MKP-1 and MKP-2 have also been found to be recently overexpressed in malignant breast cancer and gastric adenocarcinomas [56,57]. Recently, MAPK phosphatase MKP-7 has been suggested to be the tumor suppressor gene that is deleted in tumors that have chromosome 12p deletions [58].

It is believed that MKP-1 is mediating JNK expression through a parallel pathway suppressing proapoptotic signals. As this pathway is not explicitly included in our simple model of the MAPK pathway, clearly, our prediction is wrong in this case. The prediction that under-expressing MKP-1 will cause malignant transformation is a consequence of MKP-1's role as a phosphatase for ERK. This points to the obvious need for more realistic signaling networks beyond what has been developed currently. More encouragingly, such an analysis also points to the use of existing oncogene databases as a straightforward probe for discovering deficiencies in currently known signaling pathways.

There is general trend which ranks upstream members somewhat higher than downstream members. This general trend may be attributed to the general mechanism of catalysis, each upstream member phosphorylating many downstream partners and thus playing a crucial role in the transformation process. However, it is the activation of the feedback loops, particularly the control of AA, DAG and calcium, which plays the most crucial role causing cellular transformation and overcoming all the built-in attenuation processes and negative feedback mechanisms in this cellular subnetwork.

The linear response (20) of ERK to changes in expression levels is also examined (Table 7) identical to those found in Table 6, with only a few minor switches in ranking.

As oncogenic mutations are not expected to occur with single point mutations, we have extended the above analysis for multiple mutations. It is expected that mutations that

Table 7
Ranking of enzymes for overexpression and underexpression as obtained from a linear response analysis

Linear response L_i	Species overexpression	Linear response L_i	Species underexpression
0.00116	$PKC_{cytosolic}$	0.00133	PP2A
0.00066	Raf	0.00059	GAP
0.00062	Ras	0.00036	MKP1
0.00050	GEF		
0.00046	$PLA2_{cytosolic}$		
0.00032	MEK		
0.00030	GPCR		
0.00020	PLC (PIP2 binding)		
0.00019	ERK		
0.00014	PLCγ		

The values in the first and third columns are a measure of the strength of the linear response. The conclusion is the same as the previous table, viz. ERK activation is most sensitive to PKC overexpression and PP2A underexpression.

have perturbation energies that can not cause oncogenic transformation alone are capable of transforming the network when considering multiple simultaneous mutation sites. In this analysis, Fig. 3 is used again. Moreover, it is expected that even the *single* mutations described must be accompanied by corresponding mutations in regulatory pathways such as the p53 pathway [59] which would otherwise stimulate apoptosis in these mutated cells.

In the analysis of multiple mutations within the MAPK network, at each stage, several possible mutations are selected with the perturbative factor k_{mod} set for each mutation. A study of multiple simultaneous mutations using a nonlinear approach has been already performed by our group and will be presented in a forthcoming manuscript.

4. Discussion

Cancer is a cumulative process involving possibly many gene mutations [60] including those not modeled explicitly in our study such as P53 [59]. These mutations in distinct pathways are part of an interacting signaling network [2,61]. As the nature of these complex interactions are not yet fully determined, we have made a simple additive assumption in our current study. That is, the approach is designed to find genes which cause malignant transformation within the MAPK signal transduction pathway, under the assumption that all necessary genes not explicitly modeled, have also been transformed. This highly simplified additive assumption belies the actual complex nature of interactions within cell signaling. However, it is motivated in part by the importance of Ras-related mutations in tumor cells. While simplified, the computational analysis of the canonical MAPK pathway includes several major networks including PLC, PLC-γ, PLA2, PKC, Ras and calcium sequestering channels developed by Bhalla and Iyengar [11]. The interplay between the positive and negative feedback loops, attenuation and stimulatory processes all crucially govern signaling within this subnetwork [11]. As such, a computational analysis of these nonlinear interactions for putative oncogenes within this subnetwork may be of use and correlates well with experimentally available data even with this simplification.

In the current analysis, we consider elevated levels of activated ERK in the absence of EGF stimulus as an "output signal" for transcription leading to uncontrolled cell proliferation and ultimately tumor formation. This is not the only signal which triggers cell division. For instance, measuring cytochrome *C* release in the p53 pathway in the nucleus leading to apoptosis is an example of another output signal. Other interacting growth related signaling pathways, such as the PI-3K pathway or the retinoblastoma (Rb) pathway which control the cell cycle or the p53 pathway which affects apoptosis are not included in this study. As these related pathways become better quantified, it is expected that a similar analysis may elucidate what role cooperative mutations in multiple pathways play. For the current study, we make the simplification that assumes sufficient mutations that are necessary for oncogenic transformation, in addition to those modeled explicitly, have already taken place, and that this behavior is to first-order additive.

We have developed and used a nonlinear analysis method motivated by simple kinetic and energetic considerations to rank plausible oncogenes in the MAPK, PKC, PLC-γ, PLA2 and Ca^{2+} regulatory pathways using ERK phosphorylation levels as gauges of potential oncogenesis. The algorithm gauges the response of the signaling pathway to changes in the cell by measuring the lowest threshold at which a particular mutation may still cause malignant signaling. Using energetic considerations of mutations on kinetics, we reanalyze the system using a linearized procedure based on sensitivity analysis around the steady state or metabolic control analysis.

Both the direct computational approach and sensitivity analysis give rise to quantitatively rank ordered sets of mutations and changes in expression levels. They both show remarkable correlation with the current literature. In considering a single site mutation in the signaling pathway, our analysis predicts both well-known mutations as well as several novel interactions not found in the literature. The close correlation to many mutations already known in the literature lends credence to this type of analysis on simplified pathways as well as to the plausibility of several of the highly ranked predictions that are as of yet unknown.

Both specific Ras GAP mutations were highly ranked. Mutations that inhibit Ras Raf interactions, mutations in PP2-A as well as Raf were all ranked highly. Dominating the rankings, we found a clear separation between the ranking of PP2-A and the next highly ranked mutation.

Several of the mutations predicted to cause oncogenesis by over or under-expression are well known in the literature. The mutations also include several that are not known (as far as we are aware) in the literature. These include

modifications in the calcium regulatory pathway and mutations in PKC.

The analysis incorrectly predicts the behavior of MKP whose role is not entirely clear currently as it has been found to be both under- and overexpressed in tumor cells. The expression levels/mutations of GEF and ERK are also not known to be essential in tumor development.

A limitation of the current work is that not all interacting partners of these pathways are well known. Nonetheless, even with this simplified model, the quantitative predictions correlate quite well with known mutations in the literature. As new interactions are discovered and quantified, we expect to include these newly discovered pathways in this analysis. Using ERK phosphorylation level as a single gauge of malignant transformation represents a major simplification. The inclusion of other parallel pathways such as apoptotic or proliferation pathways is needed to fully gauge the transformation process. At this stage, this analysis should be considered with the qualification that if other regulatory mechanisms such as cell cycle checkpoints and decreased sensitivity to apoptosis signals have been compromised, what mutations may also be present which will cause malignant signaling to cause full-blown transformation.

As oncogenesis is a highly complex cumulative process, the single site mutations presented must be considered within a framework of additional mutations in pathways not modeled. The single mutations found in MAPK pathway should be considered to be leading indicators of mutations which are likely to be coupled to these additional mechanisms.

Acknowledgments

We would like to thank Drs. U. Rodeck and C. Kari for their discussion, insight and comments. This work was supported in part by NSF Bioinformatics Starter Grant, Pennsylvania Tobacco Health Funds Initiative and a Sun Microsystems Research Initiative Grant.

References

[1] J. Jordan, R. Iyengar, Modes of interactions between signaling pathways, Biochem. Pharmacol. 55 (1998) 1347–1352.
[2] G. Weng, U.S. Bhalla, R. Iyengar, Complexity in biological signaling systems, Science 284 (1999) 92–96.
[3] U. Krengel, L. Schlichting, A. Scherer, R. Schumann, M. Frech, J. John, W. Kabsch, E. Pai, A. Wittinghofer, Three-dimensional structures of *h-ras* p21 mutants: molecular basis for their inability to function as signal switch molecules, Cell 62 (1990) 539–548.
[4] J.L. Bos, Glowing switches, Nature 411 (2001) 1006–1007.
[5] K. Scheffzek, M. Ahmadian, W. Kabsch, L. Wiesmuller, A. Lautwein, F. Schmitz, A. Wittinghofer, The *ras*-rasgap complex: structural basis for gtpase activation and its loss in oncogenic ras mutants, Science 277 (1997) 333–338.
[6] D.J. Slamon, G.M. Clark, S.G. Wong, W.J. Levin, A. Ullrich, W.L. McGuire, Human breast cancer: correlation of relapse and survival with amplification of the her-2/neu oncogene, Science 235 (1987) 177–182.
[7] D. Nathanson, A. Culliford, J. Shia, B. Chen, M. D'Alessio, Z. Zeng, G. Nash, W. Gerald, F. Barany, P.B. Paty, Her 2/neu expression and gene amplification in colon cancer, Int. J. Cancer 105 (2003) 796–802.
[8] B. Schoeberl, C. Eichler-Jonsson, E.D. Gilles, G. Muller, Computational modeling of the dynamics of the map kinase cascade activated by surface and internalized egf receptors, Nat. Biotechnol. 20 (2002) 370–375.
[9] B. Kholodenko, Negative feedback and ultrasensivity can bring about oscillations in the mitogen-activated protein kinase cascades, Eur. J. Biochem. 267 (2000) 1488–1583.
[10] A. Levchenko, J. Bruck, P. Sternberg, Scaffold proteins may biphasically affect the levels of mitogen-activated protein kinase signaling and reduce its threshold properties, Proc. Natl. Acad. Sci. 97 (2000) 5818–5823.
[11] U.S. Bhalla, R. Iyengar, Emergent properties of networks of biological signaling pathways, Science 283 (1999) 381–387.
[12] U.S. Bhalla, P.T. Ram, R. Iyengar, Map kinase phosphatase as a locus of flexibility in a mitogen-activated protein kinase signaling network, Science 297 (2002) 1018–1023.
[13] M. Nelson, W. Hedley, http://cellml.org, cellML Bioengineering Institute Physiome Home Page (2000).
[14] J. Bower, U.S. Bhalla, D. Bilitch, E.D. Schutter, M. Hucka, V. Jagadish, M. Nelson, J. Uhley, M. Vanier, M. Wilson, http://www.genesis-sim.org/GENESIS, genesis Home Page (1988).
[15] A. Ghosh, http:// silicon.physics.drexel.edu /cellsim, cellSIM Home Page (2004).
[16] B.N. Kholodenko, A. Kiyatkin, F.J. Bruggeman, E. Sontag, H.V. Westerhoff, J.B. Hoek, Untangling the wires: a strategy to trace functional interactions in signaling and gene networks, Proc. Natl. Acad. Sci. 99 (2002) 12841–12846.
[17] B.F.J., W.H.V., K.B.N., Modular response analysis of cellular regulatory networks, J. Theor. Biol. 218 (2002) 507–520.
[18] D.G. Cacuci, Sensitivity and Uncertainty Analysis: Volume 1. Theory, Chapman & Hall, 2003.
[19] H. Kacser, J.A. Burns, The control of flux, Symp. Soc. Exp. Biol. 27 (1973) 65–104.
[20] R. Heinrich, T.A. Rapoport, A linear steady state treatment of enzymatic chains. General properties, control and effector strength, Eur. J. Biochem. 42 (1974) 89–95.
[21] C. Reder, Metabolic control theory: a structural approach, J. Theor. Biol. 135 (1988) 175–201.
[22] D.A. Fell, Metabolic control analysis: a survey of its theoretical and experimental development, Biochem. J. 286 (1992) 313–330.
[23] A.C. Bowden, Metabolic control analysis in theory and practice, Adv. Mol. Cell Biol. 11 (1995) 21–64.
[24] R. Heinrich, S. Schuster, The Regulation of Cellular Systems, Kluwer, Boston, 1996.
[25] R. Ruediger, H.T. Pham, G. Walter, Alterations in protein phosphatase 2a subunit interaction in human carcinomas of the lung and colon with mutations in the a-beta subunit gene, Oncogene 20 (2001) 1892–1899.
[26] G.A. Calin, M.G. di Iasio, E. Caprini, I. Vorechovsky, P.G. Natali, G. Sozzi, C.M. Croce, G. Barbanti-Brodano, G. Russo, M. Negrini, Low frequency of alterations of the alpha (ppp2r1a) and beta (ppp2r1b) *iso*-forms of the subunit a of the serine–threonine phosphatase 2a in human neoplasms, Oncogene 19 (2000) 1191–1195.
[27] S.S. Wang, E.D. Esplin, J.L. Li, L. Huang, A. Gazdar, J. Minna, G. Evans, Alterations of the *ppp2r1b* gene in human lung and colon cancer, Science 282 (1998) 284–287.
[28] R. Cutler, D. Morrison, Mammalian raf-1 is activated by mutations that restore raf signaling in *Drosophila*, EMBO J. 16 (1997) 1953–1960.

[29] J. Ghosh, C. Myers, Arachidonic acid stimulates prostate cancer cell growth: critical role of 5-lipoxygenase, Biochem. Biophys. Res. Commun. 235 (1997) 418–423.
[30] Y. Chen, M. Hughes-Fulford, Prostaglandin e_2 and the protein kinase a pathway mediate arachidonic acid induction of c-*fos* in human prostate cancer cells, Br. J. Cancer 82 (2000) 2000–2006.
[31] L. Levine, Does the release of arachidonic acid from cells play a role in cancer chemoprevention? FASEB J. 17 (2003) 800–802.
[32] Y. Gong, L.J. Blok, J.E. Perry, J.K. Lindzey, D.J. Tindall, Calcium regulation of androgen receptor expression in the human prostate cancer cell in lncap, Endocrinology 136 (1995) 2172–2178.
[33] J.A. Knauf, L.S. Ward, Y.E. Nikiforov, M. Nikiforova, E. Puxeddu, M. Medvedovic, T. Liron, D. Mochly-Rosen, J. Fagin, Isozyme-specific abnormalities of PKC in thyroid cancer: evidence for post-transcriptional changes in PKC epsilon, J. Clin. Endocrinol. Metab. 87 (2002) 2150–2159.
[34] X. Chen, J.A. Knauf, R. Gonsky, M. Wang, E.H. Lai, S. Chissoe, J.A. Fagin, J.R. Korenberg, From amplification to gene in thyroid cancer: a high resolution mapped bacterial–artificial–chromosome resource for cancer chromosome aberrations guides gene discovery after comparative genome hybridization, Am. J. Hum. Genet. 63 (1998) 625–637.
[35] E. Mazzoni, A. Adam, E.B. Joffe, J.A. A-Ghiso, Immortalized mammary epithelial cells overexpressing protein kinase cγ acquire a malignant phenotype and become tumorigenic in vivo, Mol. Cancer Res. 1 (2003) 776–787.
[36] M. Kobzdej, J. Matuszyk, L. Strzadala, Overexpression of *ras*, *raf* and L-*myc* but not the bcl-2 family proteins is linked with resistance to tcr-mediated apoptosis and tumorigenesis in thymic lymphomas from tcr transgenic mice, Leuk. Res. 24 (2000) 33–38.
[37] R. Mangues, J.M. Kahn, I. Seidman, A. Pellicar, An overexpressed *n*-ras proto-oncogene cooperates with *n*-methylnitrosourea in mouse mammary carcinogenesis, Cancer Res. 54 (1994) 6395–6401.
[38] J.E. Filmus, R.N. Buick, Stability of c-k-*ras* amplification during progression in a patient with adenocarcinoma of the ovary, Cancer Res. 45 (1985) 4468–4472.
[39] Z. Husain, Q.M. Yang, D.K. Biswas, Cha-ras proto-oncogene. Amplification and overexpression in UV-b induced mouse skin papillomas and carcinomas, Arch. Dermatol. 126 (1990) 324–330.
[40] Y. Kim, J.Y. Han, T.S. Kim, P.S. Kim, Y.C. Chu, Overexpression of c-h-ras p21 is correlated with vascular endothelial growth factor expression and neovascularization in advanced gastric carcinoma, J. Gastroenterol. Hepatol. 15 (2000) 1393–1399.
[41] K. Sorsdahl, A. Casson, M. Troster, D.V. Meyel, R. Inculet, A.F. Chambers, p53 and ras gene expression in human esophageal cancer and barrett's epithelium: a prospective study, Cancer Detect. Prev. 18 (1994) 179–185.
[42] C. Galiana, J.C. Lozano, B. Bancel, H. Nakazawa, H. Yamasaki, High frequency of ki-ras amplification and p53 gene mutations in adenocarcinomas of the human esophagus, Mol. Carcinog. 14 (1995) 286–293.
[43] P. Erhardt, E.J. Schremser, G.M. Cooper, B-*raf* inhibits programmed cell death downstream of cytochrome *c* release from mitochondria by activating the MEK/ERK pathway, Mol. Cell. Biol. 19 (1999) 5308–5315.
[44] J.M. Davis, P.M. Navolanic, C.R. Weinstein-Oppenheimer, L.S. Steelman, W. Hu, M. Konopleva, M.V. Blagosklonny, J.A. McCubrey, Raf-1 and bcl-2 induce distinct and common pathways that contribute to breast cancer drug resistance, Clin. Cancer Res. 9 (2003) 1161–1170.
[45] B.P. Kennedy, C. Soravia, J. Moffat, L. Xia, T. Hiruki, S. Collins, S. Gallinger, B. Bapat, Overexpression of the nonpancreatic secretory group II pla2 messenger RNA and protein in colorectal adenomas from familial adenomatous polyposis patients, Cancer Res. 58 (1998) 500–503.
[46] S. Yamashita, J. Yamashita, M. Ogawa, Overexpression of group II phospholipase a2 in human breast cancer tissues is closely associated with their malignant potency, Br. J. Cancer 69 (1994) 1166–1170.
[47] J.R. Graff, B.W. Konicek, J.A. Deddens, M. Chedid, B.M. Hurst, B. Colligan, B.L. Neubauer, H.W. Carter, J.H. Carter, Expression of group IIa secretory phospholipase a2 increases with prostate tumor grade, Clin. Cancer Res. 7 (2001) 3857–3861.
[48] M.J. Smit, D. Verzijl, P. Casarosa, M. Navis, H. Timmerman, R. Leurs, Kaposi's sarcoma-associated herpesvirus-encoded G protein-coupled receptor orf74 constitutively activates p44/p42 MAPK and AKT via GI and phospholipase *c*-dependent signaling pathways, J. Virol. 76 (2002) 1744–1752.
[49] H. Oka, Y. Chatani, R. Hoshino, O. Ogawa, Y. Kakehi, T. Terachi, Y. Okada, M. Kawaichi, M. Kohno, O. Yoshida, Constitutive activation of mitogen-activated protein (MAP) kinases in human renal cell carcinoma, Cancer Res. 55 (1995) 4182–4187.
[50] P.B. Mehta, B.L. Jenkins, L. McCarthy, L. Thilak, C.N. Robson, D.E. Neal, H.Y. Leung, MEK5 overexpression is associated with metastatic prostate cancer and stimulates proliferation, mmp-9 expression and invasion, Oncogene 22 (2003) 1381–1389.
[51] C.B. Weldon, A.B. Scandurro, K.W. Rolfe, J.L. Clayton, S. Elliott, N.N. Butler, L.I. Melnik, J. Alam, J.A. McLachlan, B.M. Jaffe, B.S. Beckman, M.E. Burow, Identification of mitogen-activated protein kinase as a chemo-resistant pathway in mcf-7 cells by using gene expression microarray, Surgery 132 (2002) 293–301.
[52] M. Marchisio, A.D. Baldassarre, D. Angelucci, E. Caramelli, A. Cataldi, S. Castorina, A. Antonucci, L. diGiovannantonio, C. Schiavone, R. diBiagio, M. Falconi, G. Zauli, S. Miscia, Phospholipase *c* δ2 expression characterizes the neoplastic transformation of the human gastric mucosa, Am. J. Pathol. 159 (2001) 803–808.
[53] J.G. Park, Y.H. Lee, S.S. Kim, K.J. Park, D.Y. Noh, S.H. Ryu, P.G. Suh, Overexpression of phospholipase *c*-gamma 1 in familial adenomatous polyposis, Cancer Res. 54 (1994) 2240–2244.
[54] Y.P. Ching, C.M. Wong, S.F. Chan, T.H. Leung, D.C. Ng, D.Y. Jin, I.O. Ng, Deleted in liver cancer (dlc) 2 encodes a rho-gap protein with growth suppressor function and is underexpressed in hepatocellular carcinoma, J. Biol. Chem. 278 (2003) 10824–10830.
[55] M. Loda, P. Capodieci, R. Mishra, H. Yao, C. Corless, W. Grigioni, Y. Wang, C. Magi-Galluzzi, P.J. Stork, Expression of mitogen-activated protein kinase phosphatase-1 in the early phases of human epithelial carcinogenesis, Am. J. Pathol. 149 (1996) 1553–1564.
[56] H.Y. Wang, Z. Cheng, C.C. Malbon, Overexpression of mitogen activated protein kinase phosphatases MKP1, MKP2 in human breast cancer, Cancer Lett. 191 (2003) 229–237.
[57] Y.J. Bang, J.H. Kwon, S.H. Kang, J.W. Kim, Y.C. Yang, Increased MAPK activity and MKP-1 overexpression in human gastric adenocarcinoma, Biochem. Biophys. Res. Commun. 250 (1998) 43–47.
[58] I. Hoornaert, P. Marynen, J. Goris, R. Sciot, M. Baens, MAPK phosphatase DUSP16/MKP-7, a candidate tumor suppressor for chromosome region 12p12–13, reduces bcr–abl-induced transformation, Oncogene 22 (2003) 7728–7736.
[59] B. Vogelstein, D. Lane, A.J. Levine, Surfing the p53 network, Nature 408 (2000) 307–310.
[60] L.A. Loeb, K.R. Loeb, J.P. Anderson, Multiple mutations and cancer, Proc. Natl. Acad. Sci. 100 (2003) 776–781.
[61] R.C. Sears, J.R. Nevins, Signaling networks that link cell proliferation and cell fate, J. Biol. Chem. 277 (2002) 11617–11620.